ISSN (Print) 1226-1750
ISSN (Online) 2233-6656
Journal of Magnetics 22(3), 478-482 (2017) https://doi.org/10.4283/JMAG.2017.22.3.478

Nuclear Magnetic Resonance Study of O-ring Polymer Exposed to High-Pressure Hydrogen

Chang Hoon Lee[1], Jae-Kap Jung[2]*, Sang Koo Jeon[2], Kwon Sang Ryu[2], and Un Bong Baek[2]

[1]*Department of Biochemical & Polymer Engineering, Chosun University, Gwangju 61452, Korea*
[2]*Center for Energy Materials Metrology, Korea Research Institute of Standards and Science, Daejeon 34113, Korea*

(Received 25 May 2017, Received in final form 4 July 2017, Accepted 17 July 2017)

Magic angle spinning (MAS) nuclear magnetic resonance (NMR) for ^{19}F and ^{1}H nuclei was used how exposure to high-pressure (70 MPa) H_2 gas affected an O-ring material. ^{19}F MAS NMR revealed that poly(vinylidenefluoride-*co*-hexafluoroprophylene) in VDF/HFP = 76.1/23.9 mol % (FKM type 1) was involved in the O-ring material. This copolymer may undergo main-chain scission and termination to -CF_2H end groups during depressurization of high-pressure H_2. Evidence for formation of additional -CF_2H end group includes a small increase in the ^{19}F MAS NMR signal at -96 ppm, and a corresponding ^{1}H MAS NMR signal at 7.1 ppm in comparison with those in the material that had not been exposed to high-pressure H_2. Neither the ^{19}F nor the ^{1}H MAS NMR showed chemical shift after exposure to H_2; this absence of response means that exposure to H_2 did not affect the structure of the polymer.

Keywords : MAS, NMR, O-ring polymer, Hydrogen pressure, chain scission, -CF_2H

1. Introduction

Hydrogen (H_2) has many advantages as a pure energy carrier, including abundance, light weight, and high energy content (142 MJ/kg), which is approximately triple that of gasoline. More importantly, combustion of H_2 releases only water vapor. On the contrary, H_2 has the disadvantages of being highly flammable and having low energy density (0.0180 MJ/L), which is four orders of magnitude lower than that of gasoline (34.8 MJ/L). Therefore, development of a method to store a large amount of H_2 reversibly and safely in a small and lightweight container has been the biggest challenge in realizing a hydrogen-based economy [1-7].

Six methods have been developed to store the hydrogen [7]: high-pressure storage, cryogenic storage, adsorption on molecular material with high surface area, interstitial absorption on host metal, chemical bonding to covalent and ionic compounds, and oxidation with reactive metals. Of these, only high-pressure and cryogenic storage are commercially available. High-pressure storage uses polymer tanks reinforced with carbon fiber, which can withstand very high pressures from 350 to 700 bar, to store a large amount of recoverable H_2. The cryogenic method uses a liquid helium refrigeration system to store H_2 at ~20 K.

Any H_2 storage method must be safe and should be delivered by appropriate technology with high fidelity. Therefore, H_2 is sealed at high pressure in a bombe made of metal or carbon fiber-reinforced polymer. Sealing is accomplished using either a metal gasket or an O-ring polymer. However, such sealing materials degrade gradually during reversible charging and discharging of high-pressure H_2. Therefore, extension of their life time is an essential challenge in the field of H_2 energy application. To accomplish this extension, the mechanism by which the polymer degrades under high-pressure H_2 gas must be understood.

Magic angle spinning (MAS) nuclear magnetic resonance (NMR) can detect and trace variations of molecular and crystalline structures, and molecular dynamic properties in solid state [8-10]. The method is useful to study solid-polymer variations caused by cycling pressurization and depressurization of H_2 gas. In this work, we investigate the effect of high-pressure H_2 on the polymer used in an O-ring using MAS NMR of ^{19}F and ^{1}H. The polymer was firstly identified from assignments of chemical shift of ^{19}F MAS NMR. The ratio of VDF and HFP comprising of the copolymer was determined from integrated areas of

*Corresponding author: Tel: +82-42-868-5759
Fax: +82-42-868-5018, e-mail: jkjung@kriss.re.kr

^{19}F MAS NMR. Powder x-ray diffraction (PXRD) was also used to discern the structural change of polymer before and after exposure to high-pressure H_2 gas. We suggest that the main chain undergoes scission and termination to -CF_2H end group during depressurization of H_2 gas, and that exposure to high-pressure H_2 did not affect the polymer's structural property or skeleton chemistry.

2. Experimental Methods

The O-ring material (VEA1049-12 O-ring P112) was purchased from PRETECH Co, Japan, and used twice for sealing under H_2 pressure of 70 MPa. Even though it was used only twice, the O-ring lost its sealing capability. For comparison of the H_2 gas effects, we tested the polymer from a fresh O-ring, from and an otherwise-identical O-ring that had been used under H_2 pressure. The MAS NMR of ^{19}F, and ^{1}H nuclei for two O-rings were performed at room temperature at the Korea Basic Science Institute (KBSI) Western Seoul Center, Republic of Korea.

^{19}F MAS NMR was measured using a 400-MHz solid-state NMR spectrometer (AVANCE III HD, Bruker, Germany) equipped with an HX CPMAS probe with a zirconia rotor (1.9 mm O.D.). ^{19}F Larmor frequency was 376.571 MHz. Each $\pi/2$ pulse was 1.6 μs wide with a spinning rate of 33 kHz. Total repetition time was 10 s. Heteronuclear dipolar decoupling was not used. ^{19}F MAS NMR FID was accumulated 16 times, then subject to fast Fourier transformation to yield spectra. LiAsF6acq (−69.5 ppm) was used as chemical-shift reference.

^{1}H MAS NMR was conducted using a CP/MAS probe with 2.5-mm-O.D. rotor on a UnityINOVA 600 (Varian, U.S.A.). Each $\pi/2$ pulse was 5 μs wide with a spinning rate of 25 kHz. Total repetition time of the pulse sequence was 5 s. Free induction decay (FID) was accumulated 16 times, then subjected to fast Fourier transformation to obtain a spectrum in the frequency domain.

Powder X-ray diffraction (PXRD) at room temperature was measured at the experimental center in Chosun University by using a model X'pert pro (PANalytical co., Netherlands). The X-ray generator setting values were 30 mA and 40 kV. The receiving slit was 3 mm. The sweep range was 80° (3.025° to 82°) at 0.030°/s.

3. Results and Discussion

To identify the O-ring material, the kind of polymer must be identified. Because most O-rings are composed of elastomers that contain either C and H, or C, H, and F, ^{19}F and ^{1}H MAS NMR is an appropriate method to discern the elastomer type.

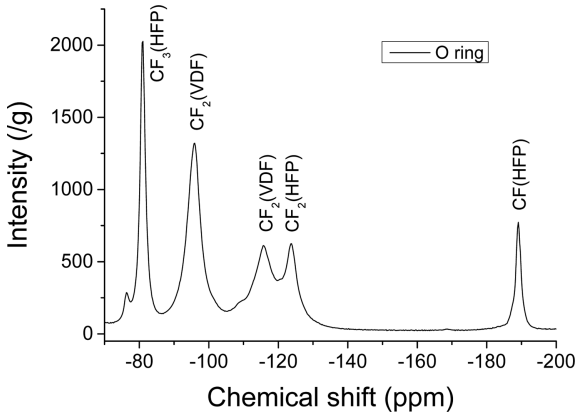

Fig. 1. ^{19}F MAS NMR spectra for fresh O-ring no use in H_2 environment at room temperature. The letter characters at maximum position indicate each chemical group responsible for the chemical shift.

A ^{19}F MAS NMR spectrum (Fig. 1) was obtained for a fresh O-ring before exposure to pressurized H_2. ^{19}F MAS NMR peaks were observed at −81, −96, −116, −124, and −189 ppm; these peaks suggest that the O-ring studied is based on a fluorinated elastomer.

According to "Standard Practice for Rubber and Rubber Lattices-Nomenclature" (ASTM D1418-05), fluorinated elastomers can be broadly classified into three groups (FKM, FFKM, and FEPM) [11]. Among them, the FKM fluoroelastomers are the largest; they consist of mostly vinylidenefluoride (VDF, CF_2=CH_2), hexafluoroprophylene (HFP, CF_2=$CF(CF_3)$), tetrafluoroethylene (TFE, CF_2=CF_2), and perfluoromethylvinylether (PMVE, CF_2=$CFOCF_3$). Some commercially-available FKM fluoroelastomers are:

1) FKM type 1: copolymers of VDF with HFP;

2) FKM type 2: terpolymers of VDF with HFP and TFE;

3) FKM type 3: terpolymers of VDF with TFE and PMVE;

4) FKM type 4: terpolymers of VDF with TFE and propylene;

5) FKM type 5: pentapolymers of VDF with HFP, TFE, PMVE and ethylene.

All of these fluoroelastomers have a VDF unit (CF_2=CH_2). Therefore, the corresponding ^{19}F MAS NMR spectrum should be observed regardless of the types. The ^{19}F MAS NMR peaks at −96 and −116 ppm (Fig. 1) match well with the chemical shifts caused by the -CF_2 group of the VDF unit, whereas the peaks at −81, −124, and −189 ppm are, respectively, compatible with CF_3, CF_2, and CF groups of the HFP unit [12-14]. These ^{19}F MAS NMR spectra obtained for the O-ring material studied are consistent with copolymers of VDF with HFP (poly(VDF-co-HFP),

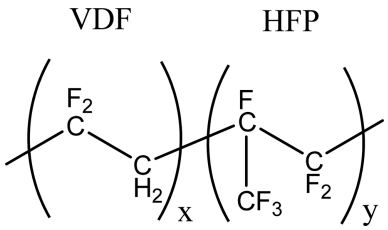

Fig. 2. Schematic representation of the molecular structure in poly(VDF-*co*-HFP) (FKM type 1).

Table 1. ^{19}F MAS NMR chemical shift assignments and fraction of integrated areas of FKM type 1 copolymer by spectral region.

Region	Chemical shift (ppm)	Chemical moiety	Origin	Integrated area
R_1	−70 to −87	CF_3	HFP	24.2
R_2	−87 to −105	CF_2	VDF	32.1
R_3	−105 to −150	CF_2	HFP, VDF	35.6
R_4	−183 to −195	CF	HFP	8.1

FKM type 1) (Fig. 2).

The ratio of VDF to HFP could be determined by comparing the integrated area of ^{19}F MAS NMR spectra by exploiting the fact that only the HFP unit contains CF_3 and CF moieties [9]. To integrate efficiently, we divide the ^{19}F spectrum in Fig. 1 into four regions: −70 to −87 ppm (R_1), −87 to −105 ppm (R_2), −105 to −150 ppm (R_3), and −183 to −195 ppm (R_4). Here, R_1 and R_4 are contributed by CF_3 and CF groups in the HFP unit, respectively, whereas R_2 and R_3 are attributed to the CF_2 group from VDF monomer and both monomer units (VDF and HFP), respectively (Table 1).

The total integrated area of CF_3 was three times larger than that of CF (Table 1). Because the integrated area at −189 ppm for CF is directly proportional to the number (#HFP) of HFP units, this relationship can be written as [12]

$$\#\mathrm{HFP} \propto I_{R4} = \frac{1}{3}(I_{R1}), \tag{1}$$

where, I_{R4} and I_{R1} are the integrated areas from R_4 and R_1 regions, respectively. For the VDF unit, because all peaks in R_2 and R_3 are attributed to the CF_2 group from both VDF and HFP, the integrated area from R_2 and R_3 divided by 2 (CF_2) should be proportional to the total number of monomer units that compromise VDF and HFP. Then the number (#VDF) of VDF units alone is proportional to the value obtained by subtracting #HFP from the total number of monomer units. Therefore,

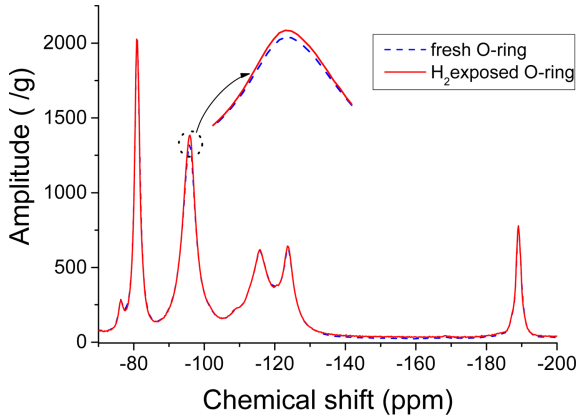

Fig. 3. (Color online) Folded representation of ^{19}F MAS NMR spectra from O-ring polymer before and after exposure to H_2 at 70 MPa. Each spectrum was normalized to its mass. Only the peak at –96 ppm increased after hydrogen exposure.

$$\#\mathrm{VDF} \propto \frac{1}{2}(I_{R2} + I_{R3}) - I_{R4}, \tag{2}$$

where I_{R2} and I_{R3} indicate the integrated areas of R_2 and R_3, respectively. Calculations using Eq. (2) and the information in Table 1 indicate that the FKM copolymer is composed of VDF/HFP = 76.1/23.9 mol %.

To quantify the H_2 effect under high pressure, ^{19}F MAS NMR measurements were obtained from an FKM copolymer exposed to high-pressure H_2 gas of 70 MPa. ^{19}F MAS NMR spectrum before and after exposure to high-pressure H_2 gas differed only in that the peak at –96 ppm for CF_2 of the VDF unit increased slightly (Fig. 3). The ^{19}F MAS NMR signal at –96 ppm originates from the -$\underline{CF_2}$- group in the sequences of –CF_2-CH_2-$\underline{CF_2}$-CH_2-CF_2- and –CF_2-CH_2-$\underline{CF_2}$-CH_2-CH_2- in the VDF unit [9, 10]. Here, the underlined CF_2 indicates a relevant ^{19}F site responsible for the peak at –96 ppm.

The natural conclusion is that the intensity increase at –96 ppm is due to an increase in the quantities of the -$\underline{CF_2}$- group in sequences of -CF_2-CH_2-$\underline{CF_2}$-CH_2-CF_2- and -CF_2-CH_2-$\underline{CF_2}$-CH_2-CH_2-. However, this result requires partial re-polymerization under high-pressure H_2. Therefore, an alternative scenario to understand the increase of intensity at –96 ppm is required. An important point is that the corresponding $\underline{CF_2}$ group is separated well by neighboring CH_2 groups; the same situation could be found in the side chain branch and at the chain end. Of these positions, the side chain branch could only be formed by polymerization process, whereas the chain end can be newly formed by scission and termination of the main chain after blooming of H_2 gas during depressurization [15].

The VDF unit can have two possible sequences: -CH_2-CF_2-, -CF_2-CH_2-; the HFP unit can also have two possible sequences: -CF_2-$CF(CF_3)$-, -$CF(CF_3)$-CF_2-, Therefore, the FKM copolymer can have four possible combinations; -CH_2-CF_2-CF_2-$CF(CF_3)$-, -CH_2-CF_2-$CF(CF_3)$-CF_2-, -CF_2-CH_2-CF_2-$CF(CF_3)$-, and -CF_2-CH_2-$CF(CF_3)$-CF_2-. In any case, scission of the main chain produces one of the radical species -$\dot{C}H_2$, -$\dot{C}F_2$, and -$\dot{C}F(CF_3)$ at the chain end; these can be immediately terminated to be -CH_3, -CF_2H, and -$CFH(CF_3)$ under H_2 atmosphere. As a result, -CH_3, -CF_2H, and -$CFH(CF_3)$ are expected to form in ratios of 0.761, 1.000, and 0.239, respectively, because our FKM copolymer has the ratio of VDF/HFP = 76.1/23.9 mol %. The –CH_3 and -$CFH(CF_3)$ moieties originated only from VDF (76.1%) and HFP (23.9%) units respectively, whereas the -CF_2H is contributed by both VDF (76.1%) and HFP (23.9%) units. Accordingly, scission of the main chain gives rise to predominant formation of -CF_2H end groups. The intensity increase of –96 ppm (Fig. 3) may be a result of an increase in the number of –CF_2H end groups by scission of the main chain.

Although ^{19}F MAS NMR signals that correspond to the chemical shifts of -C**F**$_2$H, and -C**F**H(CF_3) end groups occur at –96 ppm and –214.7 ppm, respectively, the reason that only the –96 ppm peak increases in intensity is that signal intensity at –214.7 ppm is insufficient. Correspondingly, ^1H MAS NMR spectra from the -CF_2**H** end groups should be increased. ^1H MAS NMR spectra (Fig. 4) obtained before and after exposure to H_2 gas support this suggestion well.

^1H MAS NMR spectra had two distinct peaks. The main sharp peak at 2.8 ppm can be assigned to -C**H**$_2$-, C**H**$_3$; the peak at 7.0 ppm can be assigned to the -CF_2**H** moiety in the FKM copolymer [13]. The spectra do not show any difference in meaningful chemical shift for O-ring polymer before and after exposure to high-pressure H_2 gas, but close inspection determines that the peak at 2.8 ppm of -C**H**$_2$-, C**H**$_3$ is the same within experimental error, whereas the intensity of peak at 7.0 ppm for -CF_2**H** increases. ^1H sources from the main chain breakage are -C**H**$_3$, -CF_2**H**, and -CF**H**(CF_3); of these -C**H**$_3$ and CF**H**(CF_3) occur in the range of chemical shift from 0 to 5 ppm, but the ^1H MAS NMR did not show any distinct intensity increase in this range. This absence may be due to insufficient signal intensity.

Another important point is that the chemical shift of ^1H and ^{19}F MAS NMR spectra were the same before and after exposed to high-pressure H_2 gas, indicating no variations of structural and chemical environments before and after exposed to high-pressure H_2 gas.

Powder x-ray diffraction (PXRD) was used to confirm this structural invariance before and after exposure to high-pressure H_2 gas. PXRD results (Fig. 5) show three broad peaks at $2\theta \approx 16°$, 23° and 42° and seven sharp peaks at 28°, 34°, 47°, 51°, 54°, 63° and 65°. The broad peaks may correspond to an amorphous polymer phase [16], and the sharp ones may correspond to a unknown crystalline phase in the FKM copolymer.

Because the FKM copolymer is composed of VDF/HFP = 76.1/23.9 mol %, it cannot be expected to crystallize. Accordingly, the seven sharp peaks may not originate from polymer itself but from another inorganic material. In our case, $Ca(OH)_2$ is compatible with the seven sharp peaks [15], and thus may be included as a component of

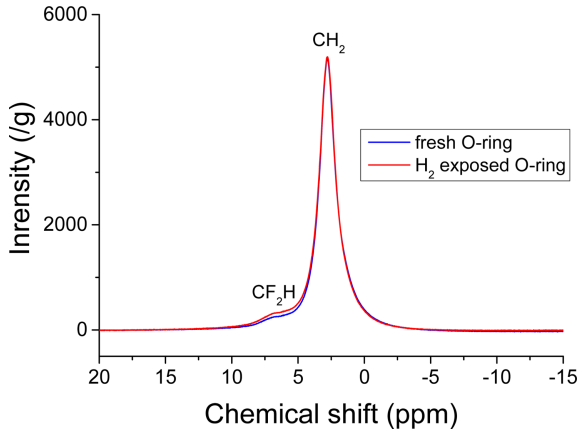

Fig. 4. (Color online) ^1H MAS NMR spectra obtained at 600 MHz for the O-ring materials before and after exposure to H_2 at 70 MPa. All spectra are normalized by their mass. Formulae at maximum positions indicate the chemical group responsible for each chemical shift.

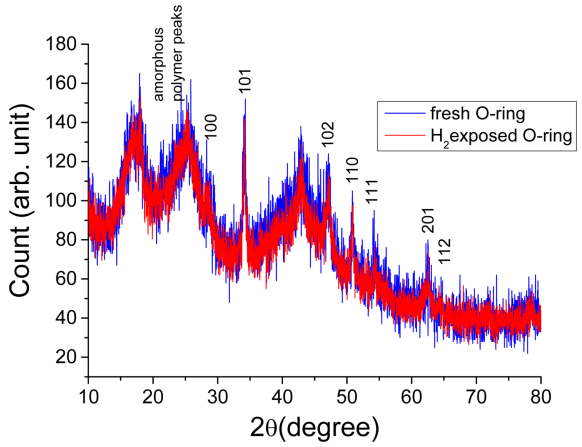

Fig. 5. (Color online) PXRD data obtained for the O-ring polymer before and after exposure to H_2 pressure of 70 MPa. Names at the maximum positions indicate the origin of each peak; Arabic sequences at maximum position are Miller indices.

the O-ring material. No variations in the peaks' position and intensities are manifested before and after exposure to high-pressure H_2 gas; i.e., exposure to high-pressure H_2 gas did not affect the crystallographic structures.

4. Conclusion

We have studied an effect of H_2 pressure of 70 MPa on an O-ring material (VEA1049-12 O-ring P112) purchased from PRETECH Co. Because we did not know the material composition of the O-ring, ^{19}F MAS NMR was first measured to discern the type of elastomer by determining whether ^{19}F nuclei are included. The strong ^{19}F MAS signal showed that the O-ring material contains fluoro-elastomers; it was identified as poly(VDF-*co*-HFP) (FKM type 1) with a ratio of VDF/HFP = 76.1/23.9 mol %.

PXRD detected diffraction patterns composed of three broad diffraction peaks that correspond well to the hollow peak from the amorphous polymer, and seven sharp peaks that correspond well to the Miller indices of $Ca(OH)_2$ crystals.

Exposure to H_2 pressure of 70 MPa did not affect the amorphous nature of the FKM copolymer or the crystalline structure of $Ca(OH)_2$, but the exposure broke part of the main chain in the FKM copolymer and terminated it with CF_2H in the process of blistering under depressurization.

Acknowledgements

This work was supported by the National Research Council of Science & Technology (NST) through development and proposal of model for polymer sealing material with withstand-hydrogen in Big Project.

References

[1] L. Schlapbach and A. Züttel, Nature **14**, 353 (2001).
[2] P. Jena, J. Phys. Chem. Lett. **2**, 206 (2011).
[3] N. Park, NAS **109**, 19893 (2012).
[4] E. Tzimas, C. Filiou, S. D. Peteves, and J.-B. Veyret, EUR-Scientific and Technical Research Reports, Mission of the Institute for Energy, European Communities 2003.
[5] A. F. Dalebrook, W. Gan, M. Grasemann, S. Moret, and G. Laurenczy, Chem. Commun. **49**, 8735 (2013).
[6] U. S. Department of Energy, https://energy.gov/eere/fuelcells/hydrogen-storage.
[7] D. J. Durbin and C. M. Jugroot, International Journal of Hydrogen Energy **38**, 15595 (2013).
[8] K. Saalwächter and H. W. Spiess, Solid-State NMR of Polymers, Polymer Science: A Comprehensive Reference **2**, 185 (2012).
[9] A. Ando, R. K. Harris, and U. Scheler, Advances in NMR, Encyclopedia of Nuclear Magnetic Resonance **9**, 531, John Wiley & Sons, Ltd, Chichester (2002).
[10] H. Fujiwara and S. Nishimura, Polym. J. **44**, 832 (2012).
[11] ASTM Standards D1418-05, ASTM International, 100 Barr Harbor Dr, West Conshohocken, PA 19428.
[12] T. J. Park, S. S. Choi, J. S. Kim, and Y. Kim, Bull. Korean Chem. Soc. **32**, 2345 (2011).
[13] E. B. Twum, Ph. D. Thesis of University of Akron, U. S. A (2013).
[14] S. Ando, R. K. Harris, G. A. Monti, and S. A. Reinsberg, Magn. Reson. Chem. **37**, 709 (1999).
[15] J. Yamabe and S. Nishimura, International Journal of Hydrogen Energy **34**, 1977 (2009).
[16] M. A. Alavi and A. Morsali, Journal of Experimental Nanoscience **5**, 93 (2010).